

Characterization of Axial Cracking Morphology of Zircaloy Cladding Tubes

G. Sanyal¹, M. K. Samal², S. Samanta³, D. K. Aswal⁴

¹Mechanical Metallurgy Division, ²Reactor Safety Division, ^{3,4}Technical Physics Division, Bhabha Atomic Research Centre; Trombay, Mumbai-400085, India

¹gsanyal@barc.gov.in; ²mksamal@yahoo.com; ³soumen.samanta@gmail.com; ⁴dkaswal@barc.gov.in

Abstract

Cladding fracture behavior is an important consideration, particularly in secondary damage of fuel cladding during service and during handling and storage of discharged fuel. Pin loading tension test is one of the most promising non-standard procedures with which quantification of initiation and propagation behavior of an axial crack of a thin-walled tubular specimen is possible. This paper focuses on characterisation of the fracture surface of a few different cladding tubes through a detailed fractographic examination and a relative comparison in crack resistance of the tubes in correlation with their fracture pattern.

Keywords

Ductile Fracture; J-R Curve; Scanning Electron Microscopy

Introduction

Zirconium-based alloys find wide application in nuclear industry for encapsulation of fuel pellets within thin-walled cladding tubes in the form of fuel pins inside the core of the water-cooled reactors for their superior properties suitable for nuclear applications. Zircaloy-2 in recrystallization annealed (RXA) condition and Zircaloy-4 in stress-relief-annealed (SRA) condition are some of the materials for fabrication of cladding tubes for the reactors in which light or heavy water acts both as coolant and moderator of neutrons. For different reactors, if such cladding tubes are fabricated from the same alloy following different processing routes, their final microstructure will be different and that may lead to difference in their in-reactor performance from the material point of view. It is important for the plant operators to ensure that the fuel pins do not burst-open under various types of operational transients as well as accident scenarios. One of the postulated design-basis accidents for the fuel-clad tubes is the reactivity initiated accident (RIA), in which, there is a sudden change in reactivity in the core. It leads to rapid heating of the ceramic fuel pellets and fission

gas release in the fuel pins. The fuel pellets expand thermally and may cause the Zircaloy clad tube to thin-down which may lead to bursting due to ductile crack propagation. In order to assess the integrity of such thin-walled tubes in these situations, the data on their fracture resistance behavior is required. For the limitations caused due to unusual geometry of such thin-walled tubes, no standard test procedure can give accurate estimate of axial crack resistance properties of the components.

Out of a few different attempts made in recent past for quantification of resistance to axial cracking, the pin loading tension (PLT) method proposed by Grigoriev et al. is found to be most promising in evaluation of axial crack resistance behavior of thin-walled tubes and using that method the authors calculated J-R curves for different thin-walled tubular components upon derivation of necessary geometric functions. Although the aspect of variation in results for different geometric parameters has been addressed to some extent, the mechanism of axial cracking with respect to variation in morphology of the fracture surface has not been studied so far. The current work is all about comparison of microstructure and cracking morphology of three different Zircaloy cladding tubes having different processing routes resulting in different degrees of resistance to axial cracking.

This paper is divided into four sections. The details of testing and characterization procedures are discussed in section II. The results are discussed with pictorial illustrations in section III followed by concluding remarks in section IV.

Experimental

Three different tubes with different tube geometry and chemical compositions are chosen for the present study. The details regarding their geometry, tensile

properties and chemical composition are elaborated in Table 1. For tubes 1 and 2, the authors have already constructed J-R curves using load normalization method after derivation of all necessary geometric functions such as $f(a/W)$,

3, the geometric functions have already been derived earlier and in the current work, construction of J-R curve is done through load normalization method and only the result is shown. The function $f(a/W)$ is important for making corrections due to finite specimen size for calculating stress intensity factor (SIF) of an axially cracked thin walled tubular specimen whereas ϕ and ψ functions are required for calculation of plastic part of J integral from experimental load-load line displacement data and making necessary updating for obtaining a crack-growth corrected J-R curve respectively.

TABLE 1 DETAILS OF GEOMETRY, TENSILE PROPERTIES AND CHEMICAL COMPOSITION OF THE THREE TUBES

Tube	Geometry		Tensile properties			
	Inner dia. (mm)	Wall thickness (mm)	Yield strength (MPa)	Ultimate tensile strength (MPa)		
Tube 1	12.4	0.9	427.6	619		
Tube 2	14.2	0.4	535	733		
Tube 3	12.3	0.38	487	615		
Tube	Chemical composition (wt %)					
	Sn	Fe	Cr	Ni	O	Zr
Tube 1	1.5	0.09	0.1	0.05	0.12	Balance
Tube 2	1.5	0.21	0.1	0.007	0.12	Balance
Tube 3	1.35	0.22	0.1	0.005	0.126	Balance



FIG. 1 AXIALLY CRACKED SPECIMEN MACHINED FROM A FUEL PIN

The appearance of a specimen fabricated from the tubes is shown in Fig. 1. The specimen is essentially a 13 mm long section cut from the tube having four coplanar notches across the tube diameter. The detailed design of the specimen is available in refs. Sufficient no. of specimens for all the three tubes is fabricated for fracture toughness testing. Based on the inner dia. of the tubes, three sets of fixtures for loading are also fabricated. A representative fixture is shown in Fig. 2. It has two symmetric halves and each half has a hemispherical mandrel. When these two halves are held together it forms a mandrel for loading of the tubular specimen in mode I fashion through insertion of pins. A more detailed description of the fixture is also available in refs. The specimens are first subjected to a set of cyclic loading steps for generation of a sharp crack ahead of the machined notch tip of length 1.5 mm. subsequently they are subjected to fracture toughness testing with different final displacements and the resultant data is analyzed upon determining crack lengths of each specimen before and after the test through a nine point averaging method under a stereomicroscope (Fig. 3). A load normalization method as per ASTM standard E-1820 is used for estimation of intermediate crack lengths and using the crack-growth information J-R curves for all three axially cracked tubes are calculated and shown in Fig. 4. More about load normalization method is available in refs..

Scanning electron microscopy of the fractured surface as well as polished and etched surface for all the three tubes are carried out. A 45% HNO_3 -45% H_2O -10% HF solution is used as etchant.

Results and Discussion

A representative picture of cracked face of a specimen is shown in Fig. 3. The length of crack extension (Δa) and the crack length prior to fracture toughness testing (a_0) are measured with nine-point averaging as described in earlier section. The portion denoted as 'crack extension' is the area of interest for study of morphology of the fracture surface. Choosing each of the specimens of the three tubes, the SEM fractography is carried out and the SEM micrograph is also separately done as described earlier.

In Fig. 4, the J-R curves for all the three tubes are compared after calculation through load normalization method. For the sake of clarity, only one curve for each tube is shown, as good reproducibility is achieved individually for all tubes considering each specimen. It is clearly seen that despite having nearly

FIG. 2 PRE-CRACKED SPECIMEN LOADED FURTHER BY TWO SPLIT MANDRELS

similar chemical composition, there is difference in crack resistance behavior of the tubes. Since concept of elastic-plastic fracture mechanics supports the fact that variation of geometry (i.e. tube wall thickness) is a governing factor in variation in strain energy release rate (J), diversity in result is evident. Still, it is important to find if there is variation in microstructure and fracture morphology that is responsible for such distinct results. Crack initiation toughness ($J_{0.2}$) of tube 3 lies between those of tube 1 and tube 2, whereas crack propagation ($\frac{dJ}{da}$) is worst for tube 3.

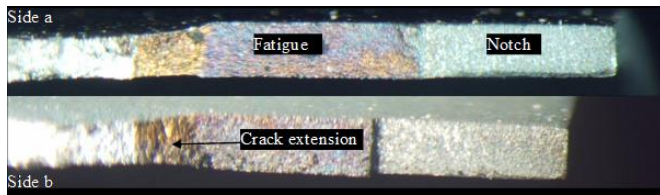


FIG. 3 FRACTURE SURFACES FOR BOTH SIDES OF THE OF A PLT SPECIMEN AFTER FRACTURE TOUGHNESS TESTING DEPICTING REGIONS OF FATIGUE PRE-CRACK AND ACTUAL CRACK PROPAGATION DURING LOADING

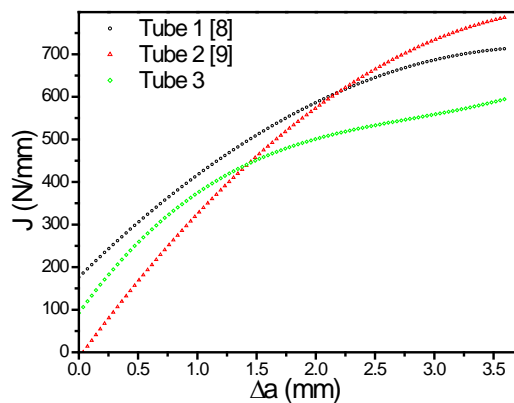


FIG. 4 THE DERIVED J-R CURVES FOR ALL THE THREE TUBES

The SEM fractographs of the cracked surface of the tubes are shown in Fig. 5-7. From comparison of the three figures, it can be inferred that different degree of prior plastic deformation is associated with initiation and propagation of crack for the tubes. The material for tube 1 is RXA Zircaloy 2 and because of recrystallization annealing there is formation of new strain-free grains, enhancing plasticity of the matrix and thus it showed a higher resistance to initiation and propagation of the axial crack if one compares with the result for tube 3. From the fractography (Fig. 5), it is seen how the ligaments surrounding any particle is stretched before complete detachment. For tube 2 and tube 3, the material that is SRA Zircaloy 4 is in stress relieved annealed condition. But still there is difference in microstructure and fractographic

appearance of the surface. From comparison between the Fig. 6 and 7 one can infer that for tube 2 the average dimple sizes are smaller and the extent to which the ligaments surrounding the dimples are stretched are also greater. Also, for tube 2, the tip of the broken ligaments is much sharper. This is why tube 2 shows superior resistance to crack propagation if compared with tube 3. Hence in a qualitative sense, it can be said that in room temperature all the three tubes show cracking behavior that comes under the purview of ductile fracture but the extent of energy absorbed during initiation and propagation of the crack are different. This is because the history of the tubes is not same. In order to find the difference in microstructure of the tubes, micrography through SEM is carried out and the micrographs of the tubes are shown in Fig. 8-10.

If one compares the sharpness of broken ligaments of the three tubes concerning axial cracking from Fig. 5-7, it can be found that it is more for tube 2 when compared with tube 1 and tube 3. From the fractographs it is evident that micro-void coalescence is perhaps the most suitable mechanism in explaining the ductile fracture associated with axial cracking of Zircaloy tubes. Micro-void coalescence is essentially a process involving three steps: (a) de-cohesion of particles embedded in the matrix under tensile load resulting in formation of tiny voids, (b) growth of the voids under prolonged loading and thinning of matrix ligament between two or three voids and finally, (c) joining of voids through complete necking and fracture of the ligaments leaving dimples at the location of the particle. In order to investigate presence of second phase particles, micrography under SEM for all the three tubes is done and the micrographs are shown in Fig. 8-10. From the three figures, it is evident that tube 1 and tube 3 have more or less same fraction of second phase particles whereas distribution and size of particles for tube 2 is different. The relative content of elements are also quantified for all the three micrographs through energy dispersive spectroscopy (EDS) confirming presence of $Zr(Cr,Fe)_2$, $Zr_2(Ni,Fe)$ type intermetallics. Tube 2 contains a larger fraction of particles in its matrix and the size of the particles is also smaller. This finding is consistent with the fractography of tube 2 presented in Fig. 6 showing a sharper appearance of the broken ligaments. The grain structure for tube 1 (Fig. 8) material is also much more revealed as it is recrystallization annealed, whereas same is not for tube 2 (Fig. 9) as is only stress relief annealed which an operation that is done at lower

temperature. The clarity of grain structure for tube 3 (Fig. 10) appears to be in between that of tube 1 and tube 2.

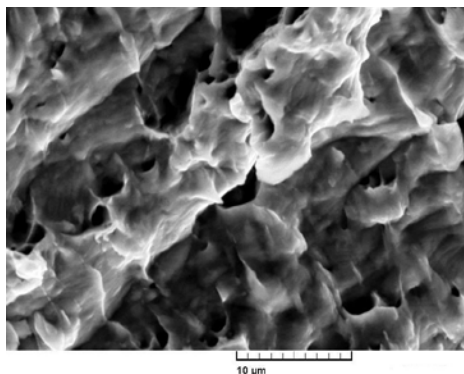


FIG. 5 SEM FRACTOGRAPH FOR TUBE 1

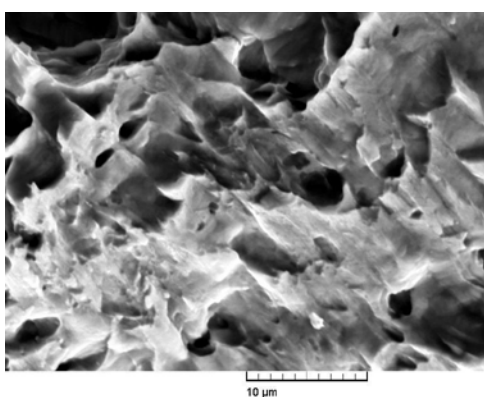


FIG. 6 SEM FRACTOGRAPH FOR TUBE 2

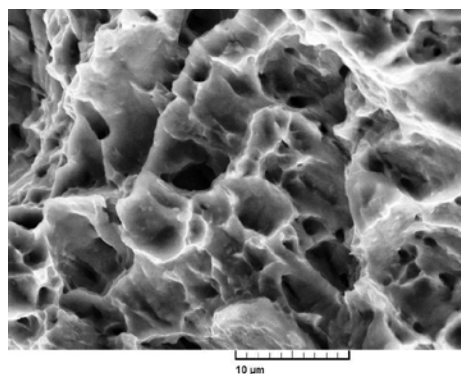


FIG. 7 SEM FRACTOGRAPH FOR TUBE 3

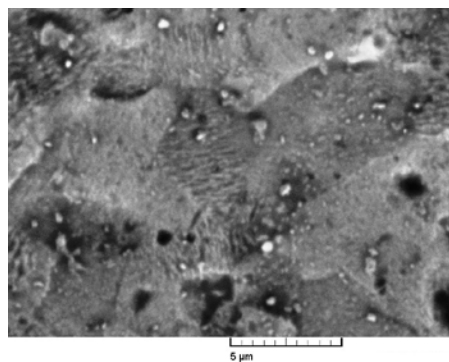


FIG. 8 SEM MICROGRAPH FOR TUBE 1

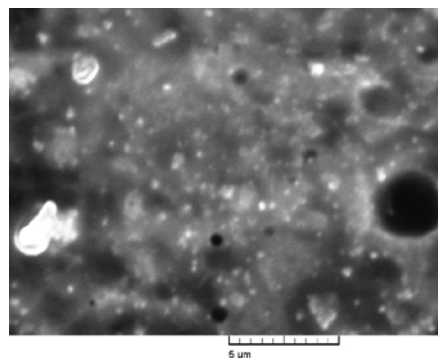


FIG. 9 SEM MICROGRAPH FOR TUBE 2

Tube 1 is fabricated starting from the as-cast Zircaloy-2 ingot through shell extrusion followed by annealing prior to three stage pilgering with intermediate recrystallization annealing. After that it is again annealed and final press pilgering is done followed by recrystallization annealing and autoclaving. During final RXA treatment, there is coarsening of the larger particles of intermetallics $Zr(Cr,Fe)_2$, $Zr_2(Ni,Fe)$ type at the expense of smaller particles.

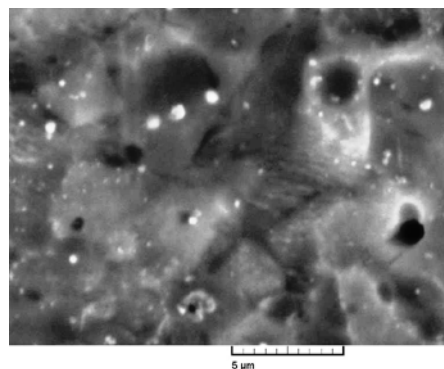


FIG. 10 SEM MICROGRAPH FOR TUBE 3

Tube 2 is fabricated starting from the as-cast Zircaloy-4 ingot by β -quenching from 1050°C. It is then hot-extruded at 825°C followed by an annealing treatment at 760°C for 4 hours. The pierced-ingot is then pilgered in three steps with intermediate recrystallization annealing at about 650°C for 4 hours between the first and second stage, and at about 575°C for 3 hours between second and third stages of cold work. The third stage of cold work is followed by stress relieving at 500°C for 10 hours.

On the other hand, for fabrication of Tube-3, the starting ingot of Zircaloy-4 is double-melted. It is then pilgered in three steps with intermediate recrystallization-annealing at about 675°C for 2 hours between the first and second, and second and third stages of the cold work process. The third stage of cold work is followed by stress relieving at 500°C for 8

hours. Thus, during the processing of the alloy for Tube-3 fabrication, all the alloying elements dissolve into the matrix and re-precipitation in the form of fine intermetallics does not occur unlike the case of material of Tube-2. In addition, the starting ingot of Tube-2 is α -quenched so that there is formation of α phase (BCC) in α phase (HCP) matrix. The α phase is more ductile compared to the α phase and it (especially, the phase-boundary) facilitates the precipitation of intermetallics. This step of heat treatment is not practiced during fabrication of the alloy of Tube-3.

Hence, microstructure, especially size and distribution of intermetallics plays a crucial role in axial crack resistance of Zircaloy cladding tubes as the dominant mechanism behind cracking of such alloy is microvoid coalescence. A little alteration in alloy chemistry and processing route may lead to great improvement in crack resistance behavior of Zr-based alloys.

Conclusions

A comparative study of axial cracking behavior of Zircaloy made cladding tubes is presented. The PLT method is suitable for calculation of J-R curves for thin-walled tubes. The cracking behavior at room temperature for the tubes is ductile in nature and apart from tube geometry it is controlled by the shape and distribution of intermetallics and strength of the base metal matrix.

ACKNOWLEDGMENT

The authors deeply acknowledge the support received from Dr. S. P. Chakraborty, Material Processing Division, Bhabha Atomic Research Centre, Mumbai, India in arranging the scanning electron microscopy facility for accomplishment of the work through interpersonal communication.

REFERENCES

- ASTM Standard E 1820-01 "Standard test method for measurement of fracture toughness" ASTM, Philadelphia, PA, 03.01: pp. 1-21, 2000.
- Bertsch, J. and Hoffelner, W., "Crack Resistance Curves Determination of Tube Cladding Material" J. Nucl. Mater., vol. 352, pp. 116-125, 2006.
- Catherine, C. Sainte, , Boulch, D. Le, S. Carassou, N. Ramasubramanian and Lemaignan, C., "An Internal Conical Mandrel Technique for Fracture Toughness Measurements on Nuclear Fuel Cladding", J. Test. Eval., vol. 34 no. 5 pp. 373-382, 2006.
- Doriot, S., Gilbon, D., Béchade, J. L., Mathon, M. H., Legras, L. and Mardon, J. P., "Microstructural Stability of M5™ Alloy Irradiated up to High Neutron Fluences", J. of ASTM Int. vol 2 no. 7 pp. 1-24, 2005.
- Edsinger, K., Davies, J.H. and Adamson, R. B., "Degraded Fuel Cladding Fractography and Fracture Behavior" pp. 316-339 in Zirconium in the Nuclear Industry: 12th International Symposium, ASTM STP 1354, G. P. Sabol and G. D. Moan, Eds., ASTM International, West Conshohocken, PA, 2000.
- Ganguly, C., "Advances in Zirconium Technology for Nuclear Reactor Application", Proc. of the Symposium Zirconim-2002 11-13 September, 2002, Bhabha atomic research Centre, Mumbai. pp. 1-27.
- Grigoriev, V., Josefsson, B. and Rosborg, B., "Fracture Toughness of Zircaloy Cladding Tubes" pp. 431-447 in Zirconium in the Nuclear Industry: 11th International Symposium, ASTM STP 1295, E. R. Bradley and G. P. Sabol, Eds., ASTM International, West Conshohocken, PA, 1996.
- Hsu H.H., Chien K.F., Chu H.C., Kuo R.C. and Liaw P.K. , "An X-Specimen Test for Determination of Thin-Walled Tube Fracture Toughness" pp. 214-226 in Fatigue and Fracture Mechanics: Vol 32, ASTM STP 1406, R. Chona, Ed., ASTM International, West Conshohocken, PA, 2001.
- Krishna, K.V.M., Sahoo, S.K., Samajdar, I., Neogy, Tewari, S., R., Srivastava, D., Dey, G.K., Das, G. H., Saibaba, N. and Banarjee, S., Mat., J. Nucl. Vol 383 pp. 78-85, 2008.
- Murai, T., Isobe, T., Mae, Y., "Polarization curves of precipitates in zirconium alloys", J. Nucl. Mat. Vol 226 pp. 327-329, 1995.
- Samal, M.K., Sanyal, G., and Chakravartty, J.K., "An experimental and numerical study of the fracture behaviour of tubular specimens in a pin-loading-tension set-up", J Mech Eng Sci vol. 224 no. 1 pp. 1-12, 2010.
- Samal, M.K., Sanyal, G., and Chakravartty, J.K., "Estimation of fracture behavior of thin walled nuclear reactor fuel pins using Pin-Loading-Tension (PLT) test", Nucl Eng Des, vol. 240 no. 12, pp. 4043-4050, 2010.
- Samal, M.K., Sanyal, G., and Chakravartty, J.K.,

“Investigation of failure behavior of two different types of Zircaloy clad tubes used as nuclear reactor fuel pins”, Engg. Fail. Anal., vol. 18no. 8 pp. 2042-2053, 2011.

Sanyal, G. and Samal, M.K., “Assessment of Axial Cracking of a Steam Generator Tube”, Journal of Metallurgical Engineering (ME) vol 1 no. 2 pp. 53-62, 2012.

Sanyal, G. and Samal, M.K., “Fracture behavior of thin-walled Zircaloy fuel clad tubes of Indian pressurized heavy water reactor”, Int. J of Frac., vol. 173no. 2, pp. 175-188, 2012.

Sanyal, G., Samal, M.K., Chakravartty, J.K., Ray, K.K., Suri, A.K. and Banerjee, S., “Prediction of J-R curves of thin-walled fuel pin specimens in a PLT setup”, Eng Fract Mech, vol. 78 no. 6, pp. 1029–1043, 2011.

Senevat, J., Pape, J. Le, Deshayes, J.F., ASTM Special Technical Publication 1132 pp. 62, 1991.



Gopal Sanyal was born in the city of Kolkata, India on March 28 in the year 1981. He is an M. Tech. (Master of Technology) in Metallurgical and Materials Engineering from Indian Institute of Technology, Kharagpur, India since 2007.

He works as a Scientist in Bhabha Atomic Research Centre, Mumbai, India since 2005. He has been working on axial cracking of thin-walled tubes and has many journal publications and book chapters in his credit pertaining to his area of interest.

Mr. Sanyal got Homi Bhabha Award for securing no. 1 rank during training examination within Metallurgy discipline prior to posting at his current job location. During undergraduate student days he was a student member of Indian Institute of Metals (IIM).



Mahendra K. Samal was born in the district of Jajpur, Orisha, India on May 3 in the year 1974. He is a PhD (Doctor of Philosophy) in Mechanical Engineering from the University of Stuttgart, Germany since 2007. In the year 2009, he also went to Ohio State University for post doctoral research.

He works as a Scientist in Bhabha Atomic Research Centre, Mumbai, India since 1996. He has immense depth of knowledge and can express his ideas well. He has plenty of areas for research and teaching, out of which finite element method, damage mechanics, online creep-fatigue monitoring, smart materials, crystal plasticity are only a few to name. He has a good amount of journal publications in his credit and edited many books, contributing very important input to scientific world.

Dr. Samal got many awards throughout his career. He received Homi Bhabha Award for ranking first among the mechanical engineers during training before absorption to his workplace. During pursuing M. Tech., he received P.M. Natu memorial prize and Ashok Chaturvedi memorial prize for ranking first in the Mechanical Engineering department of IIT Bombay. He was also selected for DAAD fellowship for carrying out Masters thesis at Technische Universität Darmstadt, Germany. He is an active teacher in Indian Nuclear Society (INS) and has affiliation with many other professional bodies.

Soumen Samanta is a Master of Science in Physics and he recently submitted his doctoral thesis for obtaining PHD degree. Mr. Samanta works in Bhabha Atomic Research Centre, Mumbai, India as a scientist since 2007. He has many publications in his credit.

Dinesh K. Aswal is a PHD in physics. Dr. Aswal works in Bhabha Atomic Research Centre, Mumbai, India as a scientist since 1987. His area of expertise covers Molecular and organic electronics, Thin films and multilayer structures, Single crystal growth, Thermoelectric devices Superconductivity etc. He has many publications in his credit.